PHYSICAL REVIEW B VOLUME 57, NUMBER 20 15 MAY 1998-II

ARTICLES

Resistivity due to low-symmetrical defects in metals

J. P. Dekker,* A. Lodder, and J. van Ek†
Faculteit Natuurkunde en Sterrenkunde, Vrije Universiteit, De Boelelaan 1081, 1081 HV Amsterdam, The Netherlands
(Received 14 November 1997)

The impurity resistivity, also known as the residual resistivity, is calculated *ab initio* using multiple-scattering theory. The mean free path is calculated by solving the Boltzmann equation iteratively. The resistivity due to low-symmetrical defects is calculated for the fcc host metals Al and Ag and the bcc transition metal V. Commonly, $1/f$ noise is attributed to the motion of such defects in a diffusion process. The results for single impurities compare well to calculations by other authors and to experimental values.
[S0163-1829(98)03820-X]

I. INTRODUCTION

The theoretical explanation for electrical resistivity is well known. Electrons move through a regular lattice of metal atoms without any resistance. As soon as irregularities are introduced into this metal, electrons are scattered, which gives rise to a finite resistivity. The temperature dependence of this quantity is mainly due to scattering of electrons by phonons. At zero temperature, when no phonons are present, the resistivity is determined by defects only, such as impurity atoms. Then it is the only remaining contribution, and therefore it is often called the residual resistivity. In this paper resistivity due to impurity atoms embedded in the metal lattice is considered, the impurity resistivity, which has been extensively studied experimentally.[1]

An interesting problem is the problem of resistance noise.[2] Over a large range of frequencies the spectral density varies as $1/f$. This can be explained, if these resistance fluctuations arise from a kind of diffusion process. In most cases the frequencies range from 1 to 1000 Hz, which correspond to typical times between jumps. The noise is attributed to a defect, which can be of any kind, jumping back and forth. A simple example of such a defect is an impurity-vacancy pair, of which we are able to calculate the resistivity for different orientations.

Many attempts have been made to calculate the impurity resistivity. The simplest methods consider an atom or a cluster of atoms embedded in free space.[3,4] More sophisticated approaches use *ab initio* methods like the Korringa-Kohn-Rostoker (KKR) theory[5–7] to describe an impurity embedded in a metal lattice. If this formalism is applied for two spin directions, magnetic impurities and materials can also be treated.[8] In most cases a substitutional or interstitial[7,9] impurity atom is considered. In this work we mainly concentrate on the resistivity due to defects, which play a role in substitutional electromigration, such as a vacancy, an impurity-vacancy pair, and an atom on its way to a neighboring vacant lattice site. The symmetry of most of the considered defects is reduced compared to a single impurity atom, which magnifies the required computational effort.

The theory, which is used to calculate the impurity resistivity, is described in Sec. II. The theory makes use of the calculation of the electron wave function described in Ref. 10, which already requires a heavy computation of a Green's-function matrix. In Sec. III, results are shown for the host metal Al. The calculations for single $3d$ and $4sp$ impurities in Al are compared with experimental and other theoretical values in Sec. III A. In Sec. III B, various calculations are reported, which are interesting in view of the reliability measurements mentioned above. Vacancies and moving host atoms in Al are considered. Resistivity calculations for impurities, a vacancy, several impurity-vacancy pairs, and an impurity at the saddle point in the fcc metal Ag are done in Sec. IV. Results from similar calculations for the bcc transition metal V are reported in Sec. V. A summary is given in Sec. VI.

II. THEORY

First the general theory will be presented. After that, some equations are given for the resistivity due to low-symmetrical defects. Finally, an expression for the generalized Friedel sum, used in the present paper, will be given. The conductivity of a sample can be calculated performing an integration over the Fermi surface,[11]

$$\sigma^{ij}=\frac{2e^2}{(2\pi)^3\hbar}\int_{\mathrm{FS}}\frac{dS_k}{v_k}v_k^i\Lambda_k^j, \tag{1}$$

in which the velocity $\mathbf{v}_k$ of an electron with quantum numbers $k\equiv(n\mathbf{k})$ is extracted from the host electronic structure. A finite electron mean free path $\mathbf{\Lambda}_k$ is due to the presence of defects or phonons, and can be calculated by solving the equation

$$\mathbf{\Lambda}_k=\tau_k^0\left[\mathbf{v}_k+\sum_{k'}\mathbf{\Lambda}_{k'}P_{k'k}\right]. \tag{2}$$

This equation follows easily from the linearized Boltzmann equation. In this paper, scattering by a static defect is con-

sidered. The defect can consist of a number of perturbed host atoms: an impurity and one or two vacancies. The probability $P_{k'k}$ for the transition through scattering from state k to k' determines the electron lifetime τ_k^0:

$$\tau_k^{0-1}=\sum_{k'} P_{k'k}. \tag{3}$$

For a low concentration c of a certain kind of defect, the transition probability $P_{k'k}$ for elastic scattering is given by

$$P_{k'k}=2\pi cN|T_{k'k}|^2\delta(\epsilon_k-\epsilon_{k'}). \tag{4}$$

The calculation of the transition matrix $T_{k'k}$ requires knowledge of the electronic wave function of the alloy. This wave function can be calculated using multiple-scattering theory. The formulation of this theory was given in Ref. 10. For the sake of clarity, some quantities appearing in the theory, which are necessary in the evaluation of the impurity resistivity, will be given here too.

The alloy wave-function coefficients c_{knL} and host wave-function coefficients c^h_{knL} are related by a matrix equation

$$c_{knL}=\sum_{n'L'} A^{nn'}_{LL'}c^h_{kn'L'}. \tag{5}$$

The matrix label n refers to an atomic site, either at a host position $\mathbf{R}_j$ or at an alloy position $\mathbf{R}_p$, and $L\equiv(l,m)$ summarizes the angular momentum labels. The matrix $A^{nn'}_{LL'}$ will be defined below. The host wave-function coefficients are evaluated at the Fermi energy $E_F=\kappa^2$, and can be written as

$$c^h_{knL}=-\frac{i^l W^0_{nL}(\mathbf{k})e^{i\mathbf{k}\cdot\mathbf{R}_n}}{\sqrt{\kappa}[-(\partial\lambda_0/\partial\epsilon_k)]^{1/2}}. \tag{6}$$

The vector $W^q_{nL}(\mathbf{k})$ is defined by

$$i^l W^q_{nL}(\mathbf{k})=\sum_{L'} b_{LL'}(\mathbf{k},\mathbf{R}_n)i^{l'}V^q_L(\mathbf{k}), \tag{7}$$

where $b(\mathbf{k},\mathbf{R}_n)$ is a lattice sum,

$$b(\mathbf{k},\mathbf{R}_n)=\sum_{j'} B(\mathbf{R}_{nj'})e^{-i\mathbf{k}\cdot\mathbf{R}_{nj'}}, \tag{8}$$

and $i^lV^q_L$ and λ^q are an eigenvector and the corresponding eigenvalue of the KKR matrix $M(\mathbf{k})=t^{h-1}-b(\mathbf{k},0)$. The matrix B is defined with Gaunt coefficients $C_{LL'L''}$ and spherical Hankel functions $h^+_L(\mathbf{r})=h^+_l(\kappa r)Y_L(\hat{r})$ as

$$B_{LL'}(\mathbf{R})=i^{l-l'-1}\kappa\sum_{L''} C_{LL'L''}i^{l''}h^+_L(\mathbf{R}). \tag{9}$$

It has to be stressed that the lattice sum in Eq. (8) extends over all host positions when $\mathbf{R}_n$ is not a host lattice position. When it is a host lattice position $\mathbf{R}_j$, the corresponding term is excluded. The $q=0$ label in Eq. (6) refers to the eigenvalue, which corresponds to a zero KKR matrix, and thereby determines the electronic structure of the metal.

The matrix $A^{nn'}_{LL'}$ in Eq. (5) is defined as[10]

$$A^{nn'}_{LL'}=\sum_{n_1L_1}(1-\mathcal{G}^{\text{void}}t)^{-1}{}^{nn_1}_{LL_1}(1-\mathcal{G}^{\text{void}}t^h)^{n_1n'}_{L_1L'}, \tag{10}$$

where the scattering matrices of the atomic host potentials t^h_n and the ones of the atomic alloy potentials t^n are calculated from their phase shifts,

$$t^n_L=-\sin(\eta_{nl})e^{i\eta_{nl}}. \tag{11}$$

The host phase shifts nd η^h_{pl} for an alloy position p are defined to be zero, if the position p does not coincide with a host position. The alloy phase shifts for the host position j are defined to be zero if the position does not coincide with an alloy position.

The formalism is made suitable to handle more general defects by making use of a void system as a reference system instead of the unperturbed host. The impurities and perturbed host atoms are replaced by free space in this reference system. The Green's-function matrix of this reference system is calculated from the host Green's-function matrix

$$\mathcal{G}^{\text{void},nn'}=\mathcal{G}^{nn'}-\sum_{j_1j_2}\mathcal{G}^{nj_1}(t^{h-1}+\mathcal{G})^{-1}_{j_1j_2}\mathcal{G}^{j_2n'}. \tag{12}$$

The host Green's-function matrix is calculated by an integration over the Brillouin zone

$$\mathcal{G}^{nn'}=\frac{1}{\Omega_{\text{BZ}}}\int_{\text{BZ}}d^3k[b(\mathbf{k},\mathbf{R}_{nn'})+b(\mathbf{k},\mathbf{R}_n)M^{-1}(\mathbf{k}) \times b^T(-\mathbf{k},\mathbf{R}_{n'})]e^{i\mathbf{k}\cdot\mathbf{R}_{nn'}}. \tag{13}$$

As derived in Refs. 7 and 12, $T_{k'k}$ can be written within multiple-scattering theory as

$$T_{k'k}=\sum_{nL} c^h_{k'nL}{}^*T^n_L c_{knL}, \tag{14}$$

where T^n_L is defined as

$$T^n_L=-\frac{1}{\kappa}\sin(\eta_{nl}-\eta^h_{nl})e^{i(\eta_{nl}-\eta^h_{nl})}. \tag{15}$$

We define an auxiliary quantity Q_{knL} as

$$Q_{knL}=\frac{i^{-l}}{\sqrt{\kappa}}T^n_L c_{knL}. \tag{16}$$

Now the sum over k' in Eq. (2) can be rewritten as a Fermi-surface integral and a set of equations in terms of $W^0_{nL}(\mathbf{k})$ and Q_{knL} can be derived straightforwardly. The equation for $\mathbf{\Lambda}_k$ becomes

$$\mathbf{\Lambda}_k=\tau^0_k\left[\mathbf{v}_k+c\sum_{nn'LL'}Q_{knL}Q^*_{kn'L'}\mathbf{I}^{nn'}_{LL'}\right], \tag{17}$$

where $\mathbf{I}$ is a Fermi-surface integral with $\mathbf{\Lambda}_k$ as a factor in the integrand

$$\mathbf{I}^{nn'}_{LL'}=\frac{2\pi}{\Omega_{\text{BZ}}}\int_{\text{FS}}dS_k\frac{W^0_{nL}(\mathbf{k})^*\mathbf{\Lambda}_kW^0_{n'L'}(\mathbf{k})}{|\nabla_k\lambda^0(\mathbf{k})|}e^{-i\mathbf{k}\cdot\mathbf{R}_{nn'}}. \tag{18}$$

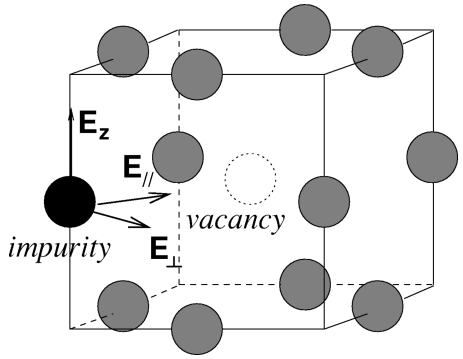

FIG. 1. Definition of the electric-field directions in the fcc structure.

Equation (17) can be solved iteratively. In the calculation of τ^0, we can make use of the optical theorem, which states that the sum over k' in Eq. (3) can be connected to the diagonal element of the transition matrix

$$\tau_k^{0-1} = -2c \ \mathrm{Im}\ T_{kk}. \tag{19}$$

The comparison of the two expressions for τ_k^0, Eqs. (3) and (19), can serve as a test for the accuracy of the Fermi-surface integrals. For a more complete description of the theory for host and alloy wave functions, the reader is referred to Ref. 10. Here we just add that an initial $\mathbf{\Lambda}$ has to be inserted in Eq. (18), e.g., $\mathbf{\Lambda}_k = \tau_k^0 \mathbf{v}_k$ or the Ziman approximation.[11] This leads to a new set of $\mathbf{\Lambda}_k$ according to Eq. (17). With this new set the integrals in Eq. (18) can be recalculated. This procedure is repeated until the set obtained equals the inserted set.

Now we give the current density-field relation for a metal containing low-symmetrical defects. In such a metal the resistivity is anisotropic, i.e., it depends on the direction of the current. Thus the relation between the electric field and the current density for, e.g., an impurity-vacancy pair in the fcc structure is given by

$$\mathbf{j} = \frac{1}{\rho\|}\mathbf{E}_\| + \frac{1}{\rho\perp}\mathbf{E}_\perp + \frac{1}{\rho z}\mathbf{E}_z, \tag{20}$$

where $\mathbf{E}_\|$ lies along the jump direction of the migrating atom, and both $\mathbf{E}_\perp$ and $\mathbf{E}_z$ are in perpendicular directions. The different directions are shown in Fig. 1. For an impurity-vacancy pair in the bcc structure there are two inequivalent directions, which are displayed in Fig. 2, and therefore the current density can be written as

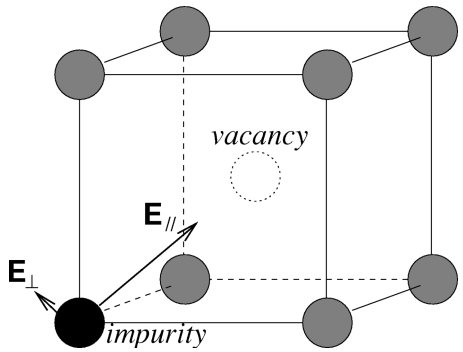

FIG. 2. Definition of the electric-field directions in the bcc structure. The directions perpendicular to $\mathbf{E}_\|$ are equivalent.

$$\mathbf{j} = \frac{1}{\rho_\|}\mathbf{E}_\| + \frac{1}{\rho_\perp}\mathbf{E}_\perp. \tag{21}$$

Equations (20) and (21) describe the current density in a sample, containing only one kind of defect, with one particular orientation. In a real sample the orientations of a defect are distributed randomly. Such a distribution results in a scalar resistivity, which is given by

$$\rho_{\mathrm{fcc}}^{-1} = \frac{1}{3}\left(\frac{1}{\rho_\|} + \frac{1}{\rho_\perp} + \frac{1}{\rho_z}\right) \tag{22}$$

for an fcc metal, and by

$$\rho_{\mathrm{bcc}}^{-1} = \frac{1}{3}\left(\frac{1}{\rho_\|} + \frac{2}{\rho_\perp}\right) \tag{23}$$

for a bcc metal.

Finally, in order to check the requirement of charge neutrality for the potentials to be used, we need an expression for the generalized Friedel sum. We will show that it is possible to derive such an expression, using the formalism presented above. According to Lodder and Braspenning[13] the electron density of states of a system $n(E)$ can be written with respect to an arbitrary reference system as

$$n(E) = n^{\mathrm{ref}}(E) + \frac{2}{\pi}\mathrm{Im}\frac{d}{dE}\mathrm{Tr}\ \ln\ T(E), \tag{24}$$

where $T(E)$ is the t matrix of the system, with respect to the reference system. Conventionally the unperturbed host has served as a reference system for a dilute alloy. For a general defect the void system serves as the natural reference system. In that case the t matrix of the system can be written as

$$T(E) = t(1 - \mathcal{G}^{\mathrm{void}}t)^{-1}. \tag{25}$$

The integrated density of states $N(E_F) = \int^{E_F} n(E)dE$ up to the Fermi energy counts the total number of electrons accommodated in the system. The difference in the number of electrons between the alloy and the host, Z_F, is found by subtracting $N^{\mathrm{host}}(E_F)$

$$\begin{aligned} Z_F &= N(E_F) - N^{\mathrm{host}}(E_F) \\ &= \frac{2}{\pi}\ \mathrm{arg\ det}\ t - \frac{2}{\pi}\ \mathrm{arg\ det}(1 - \mathcal{G}^{\mathrm{void}}t) \\ &\quad - \frac{2}{\pi}\mathrm{arg\ det}\ t^h + \frac{2}{\pi}\mathrm{arg\ det}(1 - \mathcal{G}^{\mathrm{void}}t^h), \end{aligned} \tag{26}$$

which is the generalized Friedel sum. In the case of spherically symmetric scatterers this general expression simplifies to

$$\begin{aligned} Z_F &= \frac{2}{\pi}\sum_{pl}\ (2l+1)\,\eta_l^p - \frac{2}{\pi}N_{\mathrm{cluster}}^h\sum_l\ (2l+1)\,\eta_l^h \\ &\quad - \frac{2}{\pi}\ \mathrm{arg\ det}(1 - \mathcal{G}^{\mathrm{void}}t) + \frac{2}{\pi}\mathrm{arg\ det}(1 - \mathcal{G}^{\mathrm{void}}t^h), \end{aligned} \tag{27}$$

in which N_{cluster}^h is the number of host atoms in the void region.

This expression is more general than expressions used in the past,[14] which only applied to simple substitutional and interstitial alloys for which no intermediate void reference system was needed. We will show that Eq. (27) reduces to well-established expressions applicable to those simple systems. In order to do this, it is useful to extend the sum in Eq. (12) to interstitial sites. This can be done by defining host scattering matrices for those positions as $t_I^h=0$. By that the elements of the matrix $(t^{h-1}+\mathcal{G})^{-1}=t^h(1+\mathcal{G}t^h)^{-1}$ are equal to zero, when one of the two or both indices refer to an interstitial site. The resulting matrix equation $\mathcal{G}^{\text{void}}=\mathcal{G}-\mathcal{G}(t^{h-1}+\mathcal{G})^{-1}\mathcal{G}$ contains only matrices of the same dimension, and Eq. (12) can be rewritten as

$$\mathcal{G}=(1-\mathcal{G}^{\text{void}}t^h)^{-1}\mathcal{G}^{\text{void}}. \tag{28}$$

Note that this equation can be derived directly from Eq. (12) in the case of a substitutional alloy, where only lattice sites are occupied. In the case of an interstitial impurity the matrices are enlarged due to the presence of the interstitial atom.

The addition of a nonscattering atom does not affect the host charge. This can be seen from Eq. (27), and is trivial from a physical point of view. The matrices of the third and fourth term can be multiplied, leading to

$$\begin{aligned}(1-\mathcal{G}^{\text{void}}t^h)^{-1}(1-\mathcal{G}^{\text{void}}t)&=1-(1-\mathcal{G}^{\text{void}}t^h)^{-1}\mathcal{G}^{\text{void}}(t-t^h)\\&=1-\mathcal{G}(t-t^h).\end{aligned} \tag{29}$$

Hence the Friedel sum is given by

$$Z_F=\frac{2}{\pi}\sum_{pl}(2l+1)(\eta_l^p-\eta_l^{h,p})-\frac{2}{\pi}\arg\det[1-\mathcal{G}(t-t^h)], \tag{30}$$

which has been applied in the past to substitutional[15] and interstitial[16] alloys.

III. IMPURITY RESISTIVITIES IN AL

A. 3*d* and 4*sp* impurities in Al

In this section a single $3d$ or $4sp$ impurity is considered embedded in unperturbed Al host. This means that the charge transfer to the surrounding host atoms as well as lattice distortion are neglected. Furthermore, an impurity atom has an assumed electronic configuration, which in reality may depend on its metallic environment. From Fig. 3, in which the calculated impurity resistivities are shown, it is clear that this configuration is very important. The filled circles refer to calculations in which the impurity atom has one $4s$ electron. The values indicated by filled squares are obtained for impurity atoms with two $4s$ electrons. The impurity resisitivity of atoms having two $4s$ electrons decreases with increasing atomic number, while it shows a maximum for Mn, when only one $4s$ electron is present. The experimental values,[1] indicated in the figure by asterisks, also show such a maximum, but the values are underestimated by the calculations.

The potentials used in the calculations just described do not lead to a charge neutral system, which is unphysical. The neutrality can be restored by adding a surface charge to the atomic spheres.[17] This procedure is called the shifting procedure, because it corresponds to a shift of the atomic potential by a constant energy. The charge of the system is calculated using the generalized Friedel sum expression given in Sec. II. This procedure has been applied to transition-metal impurities with the $3d^n4s^1$ electronic configuration, and to the Ca $(4s^2)$ and $4sp$ impurities. The impurity resistivities, obtained with these potentials, are given by open circles in Fig. 3. The addition of charge leads to an increase of the resistivity in all cases, except for Sc, Ge, and As. The agreement with the experimental values becomes much better. For all $4sp$ impurities, and for the transition-metal impurities with more than six $3d$ electrons, the agreement is very good.

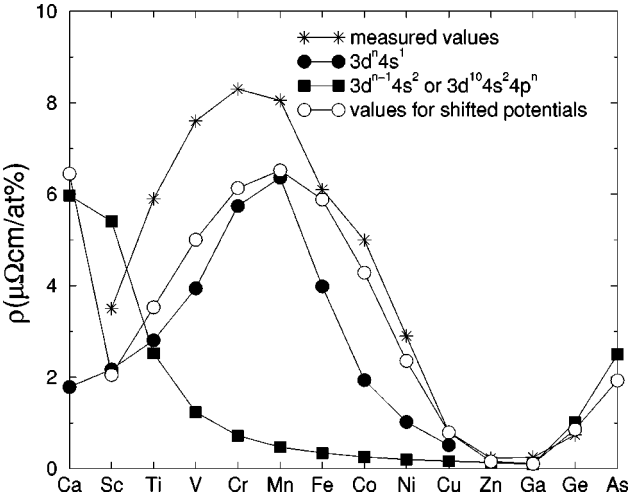

FIG. 3. Impurity resistivity of $3d$ and $4sp$ atoms in Al. For the $3d$ metals, constructed potentials are used with either one (filled circles) or two (filled squares) $4s$ electrons. Results obtained for the $4s^24p^n$ atoms are also indicated by filled squares. Open circles correspond to resistivity values obtained with shifted potentials for Ca$(4s^2)$, the $3d^n4s^1$ transition-metal atoms, and the $4p$ atoms.

The addition of surface charge is a crude attempt to simulate the effect of charge relaxation in the alloy. Still, in the case of the $3d$ impurities Fe, Co, and Ni, it enhances the accuracy of the resistivity significantly. Unfortunately, this is not the case for the other $3d$ impurities. Apparently, the surface charge does not simulate all effects of charge relaxation in the right way. Therefore it would be very interesting to repeat the calculations for Sc, Ti, V, Cr, and Mn with self-consistently calculated potentials. The method of calculation of the resistivity is not affected by the use of such potentials.

The resistivities of these impurities in Al were already calculated in Refs. 3 and 18, and recently in Ref. 4. Schöpke and Mrosan[18] used the spherical band approximation, which means that the Fermi surface is approximated by a sphere. They found resistivities, which were approximately equal to the ones following from the well-known free-electron formula of Friedel,[19] which only contains the scattering phase shifts. Just as the other authors mentioned they found an underestimation of the resistivities, which was attributed to the anisotropy of the Fermi surface. Papanikolaou, Stefanov, and Papastaikoudis[4] tried to incorporate these anisotropy effects in a tricky way and found values for the $3d$ impurities, which were too large. In our calculation this anisotropy is fully and consistently taken into account, but still the impurity resistivities are underestimated.

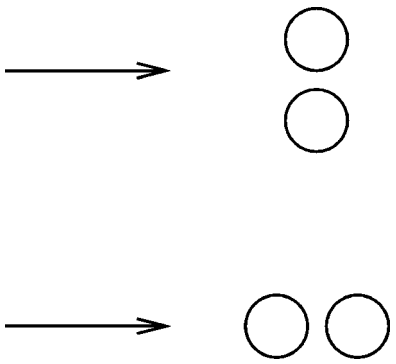

FIG. 4. Vacancy pair with two different orientations with respect to the current. The geometrical cross section is smaller when the vacancy pair is aligned with the current.

B. A migrating Al atom

According to our calculation the resistivity of a vacancy in Al is 0.57 $\mu\Omega$ cm/at. %. We used host phase shifts for all surrounding Al atoms. In first order the resistivity is the sum of the resistivities of the separate scatterers. Therefore, it is likely that the vacancy resistivity is underestimated. In the present case account of the scattering by the first shell enlarges the resistivity only slightly, to 0.60 $\mu\Omega$ cm/at. %. Our value contradicts with earlier calculations of Van Ek and Lodder[7] who found 0.93 $\mu\Omega$ cm/at. %.

The vacancy resistivity is also extracted from simultaneous measurements of the resistivity and the expansion of both the total volume and the lattice constant in an Al sample.[20] In this way a value of 3.0 $\mu\Omega$ cm/at. % is found, which is much larger than the value we found. This could have several reasons. One of the reasons can be that the electronic structure of the vacancy defect is not calculated self-consistently. From Sec. III A, indeed, a strong dependence on the electronic structure was observed. Another reason may be that the volume expansion is not entirely due to the absorption of vacancies, or that the enlargement of the resistivity is not merely due to the presence of vacancies.

During a jump the resistivity changes from the initial value, via the value at the saddle point, back to the initial value. The saddle-point value also depends on the direction of the jump with respect to the direction of the current. In the calculation a single saddle-point atom is taken into account, so scattering by the two small moon-shaped vacancies next to the atom is neglected. This procedure leads to a resistivity which is smaller than the one of the vacancy for all directions of the current, namely $\rho_{\parallel}=0.55$ $\mu\Omega$ cm/at. % and $\rho_{\perp}$ and ρ_z both have the value of 0.36 $\mu\Omega$ cm/at. %. The resistivities for the different directions are defined by Eq. (20). It is expected that the small vacancies contribute considerably to the resistivity, leading to a value, which is larger than the vacancy resistivity.

Calculations for a pair of vacancies show that the resistivity, averaged over all current directions, is equal to the resistivity of two single vacancies. Perhaps a larger cluster of perturbed host atoms or self-consistently calculated phase shifts could alter this conclusion. The symmetry of a pair is the same as the symmetry of an atom at the saddle point. Therefore, Eq. (20) holds. The parallel resistivity $\rho_{\parallel}$ turns out to be 0.94 $\mu\Omega$ cm/at. %, which is considerably smaller than the resistivity in the other two directions ($\rho_{\perp}=1.24$ $\mu\Omega$ cm/at. % and $\rho_z=1.31$ $\mu\Omega$ cm/at. %). The much smaller resistivity of a pair of vacancies aligned along the current is easily explained intuitively with the help of Fig. 4. Assuming a monotonic relation between the geometrical and scattering cross sections, the scattering cross section is obviously larger when the pair of vacancies is aligned perpendicular to the current. However, from the results for impurity-vacancy pairs, to be presented below, it follows that this intuitive, classical explanation does no justice to the quantum-mechanical character of the scattering process. Microscopically, one has to consider the scattering probability due to a pair of potentials v and w, lying at a distance $\mathbf{R}$, which, of course, is not simply equal to the sum of the individual probabilities. Even in lowest order in the potential, this probability $P_{k'k}$, calculated in the free-electron model, so using plane waves, is proportional to

$$P_{k'k}\sim v_{k'k}^2+w_{k'k}^2+2v_{k'k}w_{k'k}\cos[(k'-k).\mathbf{R}], \quad (31)$$

in which $v_{k'k}=4\pi\int r^2 dr j_0(|k'-k|r)v(r)$ is a real quantity for a spherical potential in free space. For a pair of vacancies, $v=w$. It is clear that the cosine term does not have a definite sign, and that the contribution will be different for different alignments of $\mathbf{R}$. Our results for the pair of vacancies imply that the average contribution of this term is positive for $\mathbf{R}$ perpendicular to the current, and negative for alignment along the current. For large values of $\mathbf{R}$ this term will average out, and the individual probabilities just add.

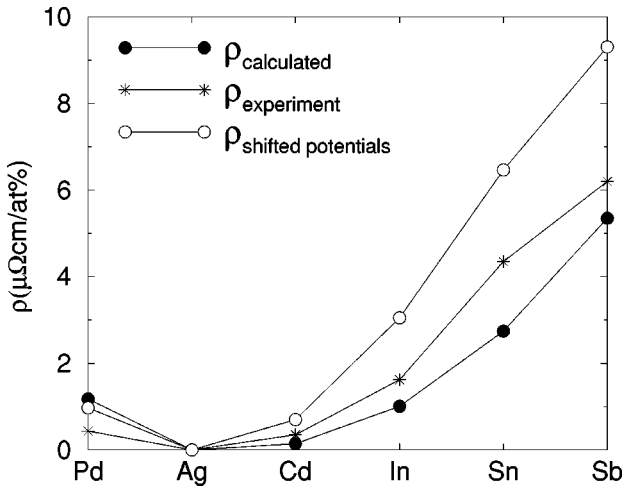

FIG. 5. Calculated and measured resistivities of $5sp$ impurities in Ag.

IV. 5SP IMPURITIES IN AG

The experimentally obtained resistivities of the $5sp$ impurities in Ag (Ref. 1) have already been used in Ref. 10 in the analysis of their wind valence. In this section the impurity resistivities will be calculated for a single impurity, an impurity next to a vacancy, and an impurity at the saddle point during a diffusion jump. In most of the calculations the perturbation of the surrounding host atoms is not taken into account. In Fig. 5, it is seen that the calculations, indicated by filled circles, and the measurements, indicated by asterisks, show the same trend. However, the measured values are larger. Only the value of 1.18 $\mu\Omega$ cm/at. % for the $4d^{10}$

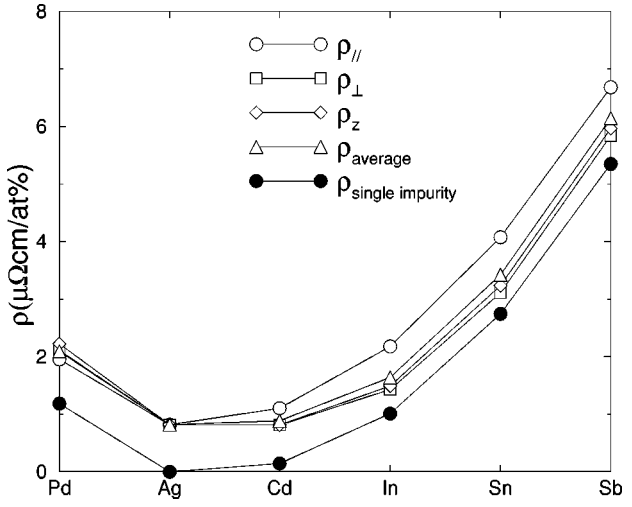

FIG. 6. Calculated resistivities of pairs of a $5sp$ impurity and a vacancy in Ag. The resistivities of the single impurities are given for comparison.

impurity Pd is an overestimation. A much lower value of 0.02 $\mu\Omega$ cm/at. % is found, when a $4d^9 5s^1$ electronic configuration is used for the Pd atom. The experimental value of 0.44 $\mu\Omega$ cm/at. % lies between the two theoretical values, which suggests that the electronic configuration is a mixture of both. The calculated resistivities are only slightly affected by taking into account a shell of perturbed host atoms. A maximum increase of 0.04 $\mu\Omega$ cm/at. % is found for In.

The shifting procedure to achieve charge neutrality is also applied in this case. The missing charge had to be added to the impurity. The resulting values are indicated by open circles in Fig. 5. Just as in the case of impurities in Al, the resistivities are enlarged. However, the agreement with experiment does not improve in this case, because the enlargement is too strong.

Similar calculations were performed in Ref. 6 using self-consistent single-site potentials. These results are comparable to ours, but they agree somewhat better with the experimental values. This could be the result of the larger muffin-tin radius that the authors used. Our muffin-tin radius is bounded, because of the decreased space at the saddle point. Nevertheless our values are reasonable.

The resistivities for $5sp$ impurity-vacancy pairs are given in Fig. 6. The resistivity for a single vacancy is 0.82 $\mu\Omega$ cm/at. %, which is the value for Ag in the figure. The resistivity of an impurity-vacancy pair, being aligned with the current, $\rho_\parallel$, is larger than the resistivity, when they are aligned perpendicular to the current, $\rho_\perp$ and ρ_z. This is in contradiction to the intuitive explanation for the resistivity of a vacancy pair in Al in the different directions in terms of a geometrical cross section, which is given in Sec. III B and illustrated in Fig. 4. However, this behavior can be understood from the simple expression (31). The impurity potential w is certainly attractive, which corresponds to an overall negative sign, and a vacancy potential v is repulsive. So, on the average, the cosine term in Eq. (31) has the opposite sign compared with the scattering by two vacancies. This implies a conversion of the behavior, in agreement with or finding for the impurity-vacancy pair. Notice also that the resistivity of an impurity-vacancy pair, averaged over all current directions, ρ_{average}, does not equal the sum of the separate resistivities of vacancy and impurity. The latter sum rather equals $\rho_\parallel$.

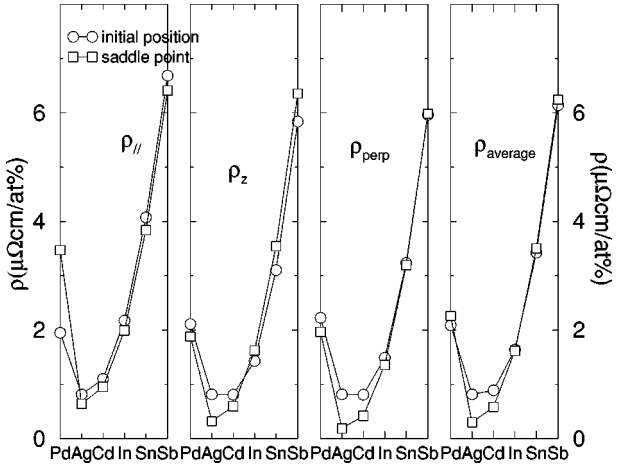

FIG. 7. Calculated resistivities in Ag of $5sp$ impurities, located next to a vacancy (initial position) and at the saddle-point position.

In Fig. 7 the impurity resistivities at the saddle point for the different current directions are compared with the corresponding resistivities for the impurity-vacancy pair. The saddle-point resistivity roughly follows the one at the initial position. Again $\rho_\parallel$ is the largest, but for an atom at the saddle point the cross section is not expected to depend strongly on the direction, because the current ''sees'' one scattering atom from all directions. Just as in the case of Al, the two small moon-shaped vacancies around the saddle-point atom are not taken into account, which is expected to lead to an underestimation of the resistivity.

V. TRANSITION-METAL IMPURITIES IN V

The measured resistivities of the $3d$ impurities Ti and Cr,[1] and the calculated ones of Sc, Ti, Cr, and Mn in V, are given in Fig. 8. The calculated values are lower than the experimental values, although the value for Cr lies fairly close. The Mn resistivity is much larger than the other ones. The value measured for the $5d$ impurity Ta of 1.5 $\mu\Omega$ cm/at. % is very

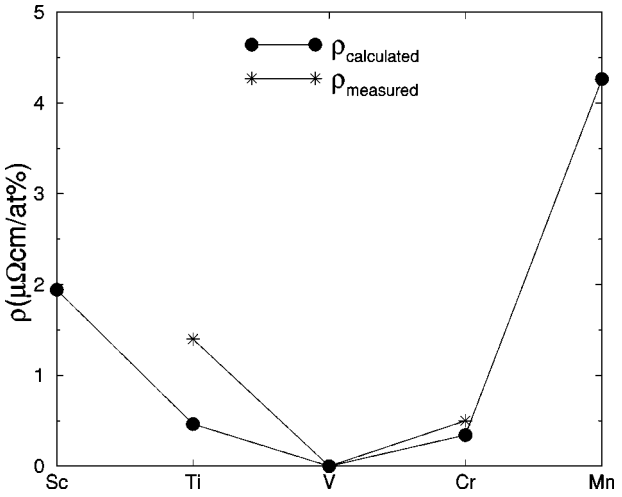

FIG. 8. Calculated and measured resistivities of $3d$ impurities in Vanadium.

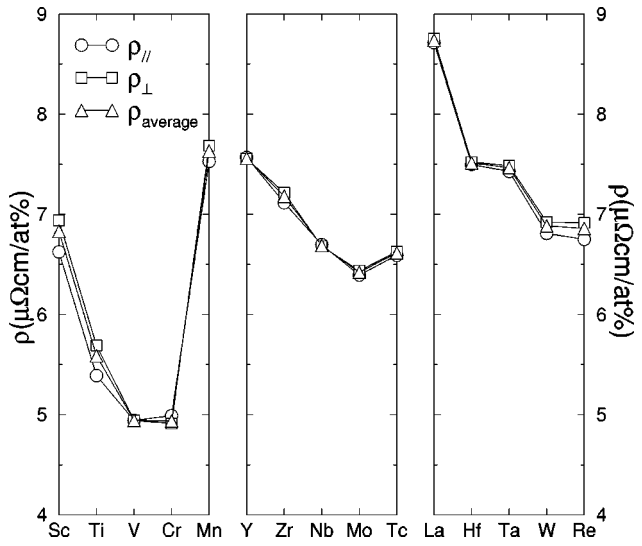

FIG. 9. Calculated resistivities of $3d$, $4d$, and $5d$ impurities, located next to a vacancy in V.

close to the calculated value of 1.3 $\mu\Omega$ cm/at. %.

The calculated resistivity of a vacancy in V is larger than of any of the $3d$ impurities, namely, 4.94 $\mu\Omega$ cm/at. %. This results in resistivities of impurity-vacancy pairs, varying from 5 to 9 $\mu\Omega$ cm/at. %, as can be seen from Fig. 9. The large value for the Mn impurity is also seen in the $3d$ series in the left panel of the figure, but the effect is not as pronounced as in the case of a single impurity. The resistivity turns out to be fairly isotropic, i.e., $\rho_{\parallel} \approx \rho_{\perp}$ in Eq. (21).

It is seen that the resistivity of a $4d$ impurity next to a vacancy tends to be larger than that of a $3d$ impurity and smaller than that of a $5d$ impurity. The resistivity for the $3d$ impurities is the lowest for V, while for the $4d$ impurities it is lowest for Mo, which has an additional valence electron. For the $5d$ impurities the resistivity of the impurity-vacancy pair decreases monotonically with the atomic number.

The resistivities for impurities at the saddle point are depicted in Fig. 10. They show a larger anisotropy. Exceptions are Cr, Mo, and W. Apart from the high value of Cr, the resistivity seems to decrease monotonically in all three series. The low value for Mn is striking in view of the high values for the single impurity and the impurity-vacancy pair. The saddle-point resistivities are larger than the initial point values. The small vacancies on either side of the atom could even enhance this effect.

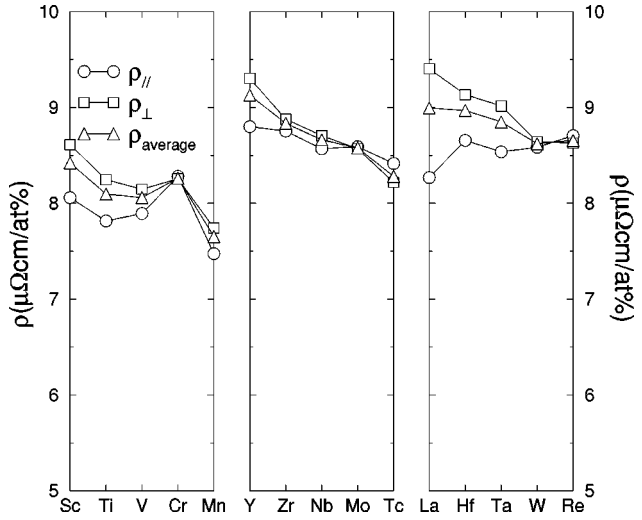

FIG. 10. Calculated resistivities of $3d$, $4d$, and $5d$ impurities, located at the saddle-point position in V.

VI. SUMMARY

In this paper a multiple-scattering method has been described for the calculation of the impurity resistivity. It makes use of the calculated wave function coefficients, introduced in Ref. 10. The linearized Boltzmann equation can be solved iteratively. One iteration step involves the calculation of a Fermi-surface integral. The integrand is the product of the vector mean free path, which depends on the crystal momentum, and two host wave-function coefficients. In its present formulation, the method is suitable to handle complicated defects such as an atom during a diffusion jump. It has been used to calculate the resistivity due to impurities, vacancies and pair defects in Al, Ag, and V.

The resistivities of $3d$ and $4sp$ impurities in Al have been calculated, basically in order to see if the calculations make sense. This series of impurities was investigated before by several authors,[18,3,4] and experimental values are available.[1] Their calculated resistivities turned out to depend strongly on the atomic electronic configuration, which is used to construct the crystal potential of the alloy. This is especially important for transition-metal impurities, where, e.g., the energies of $3d$ and $4s$ levels are almost equal. In this series it is seen that the resistivity decreases with atomic number, when the impurity has two $4s$ electrons. The shape of the experimentally observed peak is reproduced, when the impurity carries one $4s$ electron.

Another consequence of the construction of the potentials, the lack of charge neutrality, can be repaired by adding surface charge to the atomic sphere of the impurity. This procedure enlarges most calculated values, and improves the agreement with experiments. Especially for transition-metal atoms with many d electrons, and for $4sp$ impurities, the agreement becomes very good. Apparently the calculation takes the essential features of the scattering process into account. The strong dependence on the electronic configuration as well as on the addition of surface charge make it interesting to use self-consistent potentials in our calculation.

A vacancy plays an important role in the diffusion process. Its calculated resistivity in Al of 0.6 $\mu\Omega$ cm/at. % is much smaller than the experimentally obtained value of 3 $\mu\Omega$ cm/at. %. The resistivity of a host Al atom, halfway along its jump path to a neighboring vacant site, depends on the direction of the electrical current, and it is different from its value for the atom at its initial position. Both the direction and position dependence give rise to fluctuations in the resistivity on a time scale of 10^{-13} s. The value of 0.41 $\mu\Omega$ cm/at. %, which is the average over all current directions, is smaller than the value at the initial position, the latter being equal to the resistivity of a vacancy. In this calculation the two small moon-shaped vacancies next to the jumping atom are not taken into account, and it is expectable that they will enlarge the resistivity. The resistivity of a pair of vacancies depends on the direction of the current. If the

pair is aligned with the current, the resistivity is smallest. This can be attributed to a smaller cross section for such a configuration. If the resistivity is averaged over all current directions, it equals the resistivity of two single ones.

The calculated resistivities due to the $5sp$ impurities in Ag show a similar dependence on atomic number as the experimental values.[21] Just as for impurities in Al, the resistivities are underestimated. However, after achieving charge neutrality by adding a surface charge to the impurity, they become too large. The resistivity due to an impurity-vacancy pair is smaller than the sum of the impurity and vacancy resistivities. When the pair is aligned with the current, the resistivity is largest and approximately equals that sum. The fact that the resistivity is largest in that direction is in contradiction with the smaller geometrical cross section. An impurity halfway along its jump path has a larger resistivity than the impurity-vacancy pair in spite of the neglected small vacancies.

The calculated resistivities of the impurities Cr and Ta in the bcc transition metal V agree fairly well with experiment, while the resistivity of Ti is underestimated. The values for a d impurity-vacancy pair and an impurity halfway along its jump path are larger than the ones for a single impurity.

In conclusion, it has been shown that the resistivity due to low-symmetrical defects can be calculated accurately. The calculated impurity resistivities compare reasonably well with the available experimental material. They may even improve when self-consistent potentials for the alloy are used.

ACKNOWLEDGMENTS

This work was sponsored by the National Computing Facilities Foundation (NCF) for the use of supercomputer facilities, with financial support from the Nederlandse Organisatie voor Wetenschappelijk Onderzoek (Netherlands Organization for Scientific Research, NWO). The authors wish to acknowledge the contribution of P. J. Harte to a well-designed computer program for the calculation of the impurity resistivity.

*Present address: Max-Planck-Institut für Metallforschung, Seestr. 92, D-70174 Stuttgart, Germany.

†Present address: Seagate Technology, 7801 Computer Avenue South, Bloomington, MN 55435.

[1] J. Bass, in *Metals: Electronic Transport Phenomena*, edited by K.-H. Hellwege and J. L. Olsen, Landolt-Börnstein, New Series, Group III, Vol. 15, Pt. a (Springer-Verlag, Berlin, 1982).

[2] P. Dutta and P. M. Horn, Rev. Mod. Phys. **53**, 497 (1981).

[3] P. M. Boerrigter, A. Lodder, and J. Molenaar, Phys. Status Solidi B **119**, K91 (1983).

[4] N. Papanikolaou, N. Stefanou, and C. Papastaikoudis, Phys. Rev. B **49**, 16 117 (1994).

[5] I. Mertig, E. Mrosan, and P. Ziesche, in *Multiple Scattering Theory of Point Defects in Metals: Electronic Properties*, edited by W. Ebeling, W. Meling, A. Uhlmann, and B. Wilhelmi (Teubner, Leipzig, 1987).

[6] T. Vojta, I. Mertig, and R. Zeller, Phys. Rev. B **46**, 15 761 (1992).

[7] J. van Ek and A. Lodder, J. Phys.: Condens. Matter **3**, 7363 (1991).

[8] I. Mertig, R. Zeller, and P. H. Dederichs, Phys. Rev. B **47**, 16 178 (1993).

[9] J. van Ek and A. Lodder, J. Alloys Compd. **185**, 207 (1992).

[10] J. P. Dekker, A. Lodder, and J. van Ek, Phys. Rev. B **56**, 12 167 (1997).

[11] J. M. Ziman, in *Principles of the Theory of Solids*, edited by J. M. Ziman (Cambridge University Press, Cambridge, 1972).

[12] A. Lodder and J. P. Dekker, in *Proceedings of the First International Alloy Conference, Athens, 1996*, edited by A. Gonis, A. Meike, and P. E. A. Turchi (Plenum, New York, 1997), pp. 467–477.

[13] A. Lodder and P. J. Braspenning, Phys. Rev. B **49**, 10 215 (1994).

[14] For a review, see A. Lodder and J. P. Dekker, Phys. Rev. B **49**, 10 206 (1994).

[15] J. Molenaar, A. Lodder, and P. T. Coleridge, J. Phys. F **13**, 839 (1983).

[16] P. M. Oppeneer and A. Lodder, J. Phys. F **17**, 1901 (1987).

[17] R. H. Lasseter and P. Soven, Phys. Rev. B **8**, 2476 (1973).

[18] R. Schöpke and E. Mrosan, Phys. Status Solidi B **90**, K95 (1978).

[19] J. Friedel, Nuovo Cimento Suppl. **7**, 287 (1958).

[20] R. O. Simmons and R. W. Balluffi, Phys. Rev. **117**, 62 (1960).

[21] Calculations of the electromigration wind force for this series of impurities in Ag were published previously in Ref. 10.